Electroactive trilayer actuators taking advantage of the ionic conductivity and self-adhesion of ionic liquid plasticized starch

C. Catry, Denis Lourdin, G. Roelens, Giao T.M. Nguyen, Cédric Plesse, Eric Leroy, Frédéric Vidal

Carbohydrate Polymer Technologies and Applications 5 (2023) 100295

Contents lists available at ScienceDirect

Carbohydrate Polymer Technologies and Applications

journal homepage: www.sciencedirect.com/journal/carbohydrate-polymer-technologies-and-applications

Electroactive trilayer actuators taking advantage of the ionic conductivity and self-adhesion of ionic liquid plasticized starch

C. Catry [a,b], D. Lourdin [a], G. Roelens [b], Giao T.M. Nguyen [c], Frédéric Vidal [c], Cédric Plesse [c], E. Leroy [b,*]

[a] Biopolymers Interactions Assemblies Research Unit 1268 (BIA), INRAE, Rue de la Géraudière, 44316, Nantes, France
[b] Université de Nantes. Oniris. CNRS. GEPEA. UMR 6144, 44600 Saint Nazaire, France
[c] CY Cergy Paris Université, LPPI, 5 mail Gay Lussac, 95000, Cergy, France

ARTICLE INFO

Keywords:
Starch
Amylose
Ionic liquids
Electroactive
Sensors
Actuators

ABSTRACT

Ionic liquid (IL) plasticized potato starch and pure amylose films are used as Ionically Conductive Polymers (ICP) for manufacturing electroactive polymer trilayer films able to change of shape upon electrical stimulus, and to work as motion sensors. This promising alternative to fossil fuel based ICPs takes advantage of the water solubility of the starch/IL mixture and its stickiness after casting as films, allowing the design of a solvent free, origami inspired process for its assembly with PEDOT:PSS electrodes.

Electroactive free bending motions with an amplitude of deformation $\Delta\varepsilon$ of 0.45% are observed upon $\pm$ 2 V electrical stimulus for all EAPs, with a 7-fold higher blocking force for the pure amylose based system making it able to lift more than 180 times its weight.

Conversely, when tested as sensors, a 4-fold higher sensitivity is observed for the potato starch based EAP, which was comparable to that of fossil-fuel based polymers systems.

1. Introduction

Electroactive polymers (EAP) are materials able to change of shape and size upon electrical stimulus, considered as precursors of artificial muscles (Bar-Cohen, 2002; Bar-Cohen & Zhang, 2008; Bar-Cohen & Anderson, 2019; Mirfakhrai et al., 2007). Among them, ionic EAPs based on electronically conducting polymers (ECP) present the advantages of being biocompatible and activated under low voltage (< 2 V) (Melling et al., 2019): ECPs can change their volume under electrochemical stimulation thanks to the insertion/expulsion of ions during a change of oxidation level (Fig. 1**a**). Typically, the positive charges created along the ECP backbone during oxidation will promote ion motion in order to preserve electroneutrality of the system, resulting in a volume expansion or contraction, reversible upon reduction of the ECP toward its neutral state. The development of actuators operating in open-air usually involves a trilayer configuration. In this case, two ECP layers, acting respectively and alternately as anode and cathode, are sandwiching an Ionically Conductive Polymer (ICP) layer, acting as the source of ions. During electrochemical stimulation, each ECP electrode of this structure is undergoing opposite volume variation and a bending deformation is obtained. Such electrochemomechanical devices can also work as soft mechanical sensors converting a mechanical stimulation into an electric signal, and have been extensively studied for applications in soft robotics, biomedical devices and more recently wearables (Melling et al., 2019; Maziz et al., 2017).

Thermoplastic starch (TPS) based ICPs were first obtained by thermoplasticization with glycerol doped with metal salts inducing ionic conductivity (V. L. Finkenstadt & Willett, 2004; Ma et al., 2006). More recently, ionic liquid (IL) plasticized TPS was produced by casting from aqueous solutions (Wang et al., 2009), by extrusion (Sankri et al., 2010), or hot-pressing (Zhang et al., 2017). In presence of water, maximum ionic conductivities values up to a few hundredths of S.cm^{-1} have been reported for both systems (Ma et al., 2006; Wang et al., 2009; Zhang et al., 2017). However much higher water and ion contents were required for glycerol/metal salt ($\approx 10^{-2}$ S cm^{-1} at 40-50 wt.% water for 0.22 mol of glycerol, and 0.6 mol of salt per 100 g of starch (Ma et al., 2006)) than for ILs (2.5×10^{-2} S cm^{-1} at 14.5 wt. % water for 0.19 mol of 1-Allyl-3-methylimidazolium chloride ([Amim][Cl]) per 100 g of starch (Wang et al., 2009); and $1{,}2 \times 10^{-2}$ S cm^{-1} at 26 wt.% water for 0.41 mol of 1-Ethyl-3-methylimidazolium acetate ([Emim][Ace]) per

* Corresponding author.
E-mail address: eric.leroy@univ-nantes.fr (E. Leroy).

https://doi.org/10.1016/j.carpta.2023.100295

Available online 16 February 2023

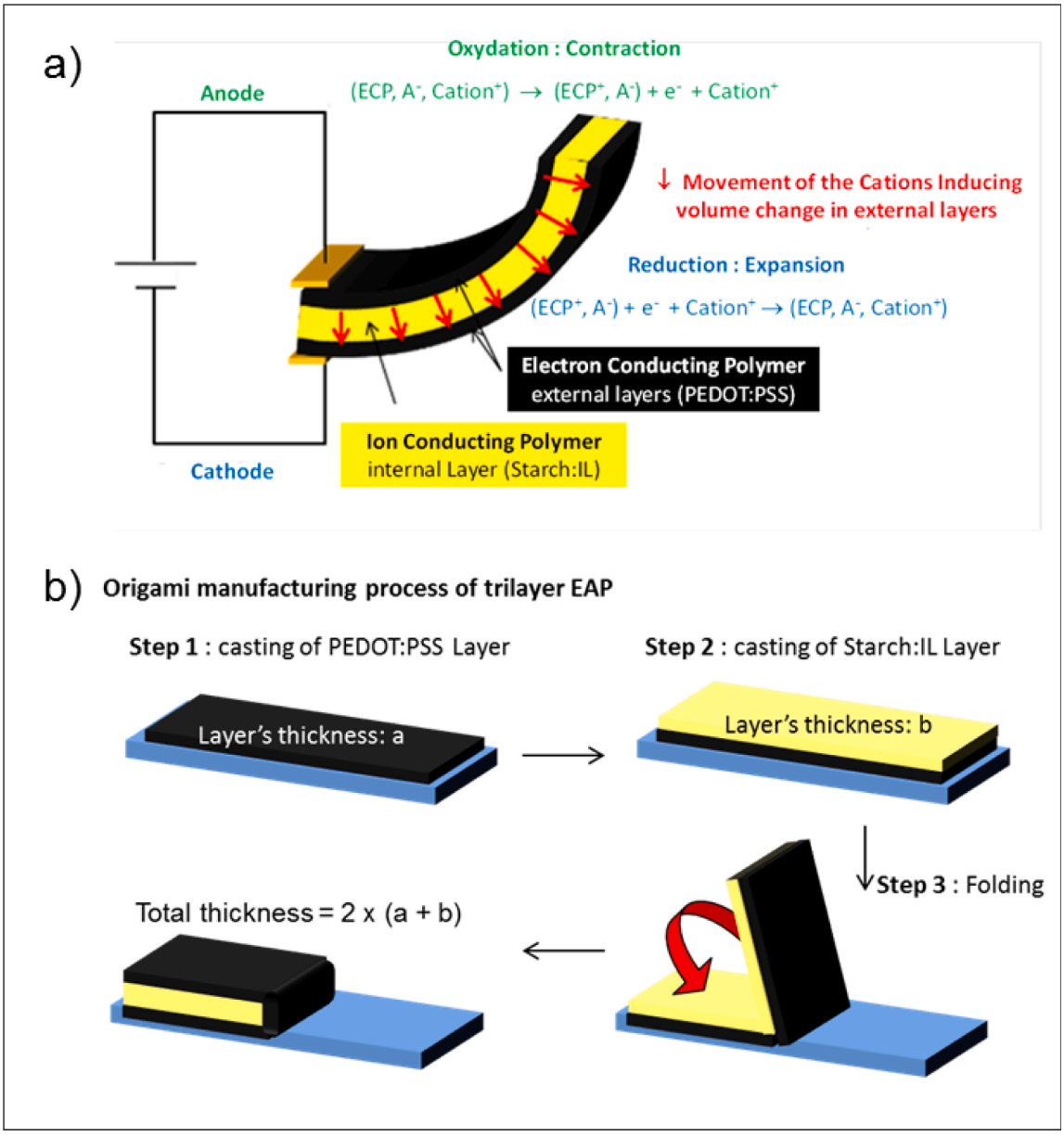

Fig. 1. Electroactive polymer trilayer actuators: **a)** General deformation mechanism under electric stimulus; **b)** Origami manufacturing process for (PEDOT:PSS) / (Starch:IL) /(PEDOT:PSS) systems.

100g of starch (Zhang et al., 2017).) Moreover, in the case of [Amim][Cl] it was reported that it prevents starch retrogradation (Zhao et al., 2015), which should be an advantage for the stability of the ICP.

Though the idea that these developments would lead to starch based EAPs was proposed two decades ago (V. L. Finkenstadt, 2005; V. Finkenstadt & Willett, 2005; V. L. Finkenstadt & Willett, 2004), this became a reality only recently (Núñez D et al., 2016): The internal ICP layer was a water cast film composed of cassava starch (27 wt.%) crosslinked with glutaraldehyde (18 wt.%), plasticized with glycerol (27 wt.%) and doped with a lithium salt ($LiClO_4$, 27 wt.%). It was combined with polypyrrole films as external ECP layers. The resulting EAP can actuate to positive and negative deformations in air upon one electrical stimulus cycle (+2 V during 20 s / -2 V during 40 s).

Among other ECPs that may be combined with starch based ICPs, the blend of poly(3,4-ethylenedioxythiophene) with poly(styrene sulfonate) (PEDOT:PSS, Fig. 2) is probably more versatile. It is actually among the most studied ECPs nowadays due to its stability in air and its availability in a commercial aqueous suspension, allowing to easily produce thin films by casting (Groenendaal et al., 2000). While the pristine electronic conductivity of PEDOT:PSS is approximately 1 S cm^{-1}, it can be increased by selective dissolution of the insulating PSS chains, thus increasing the conducting PEDOT content, with reported conductivity increase up to 1000 S cm^{-1} (Alemu et al., 2012). Last but not least, it was reported that when mixing PEDOT with starch, interactions between the two polymer take place (Arrieta et al., 2018), suggesting a compatibility that may favor cohesion between a starch based ICP and PEDOT:PSS.

In the present work, our hypothesis statement is that [Amim][Cl] IL plasticized thermoplastic starch (IL-TPS) can be used as an ICP in trilayer air working ionic EAPs, in combination with ECP layers are based on PEDOT:PSS. We will describe the manufacturing process of such assemblies, and the assessment of their electroactive properties for potential applications as actuators and as sensors.

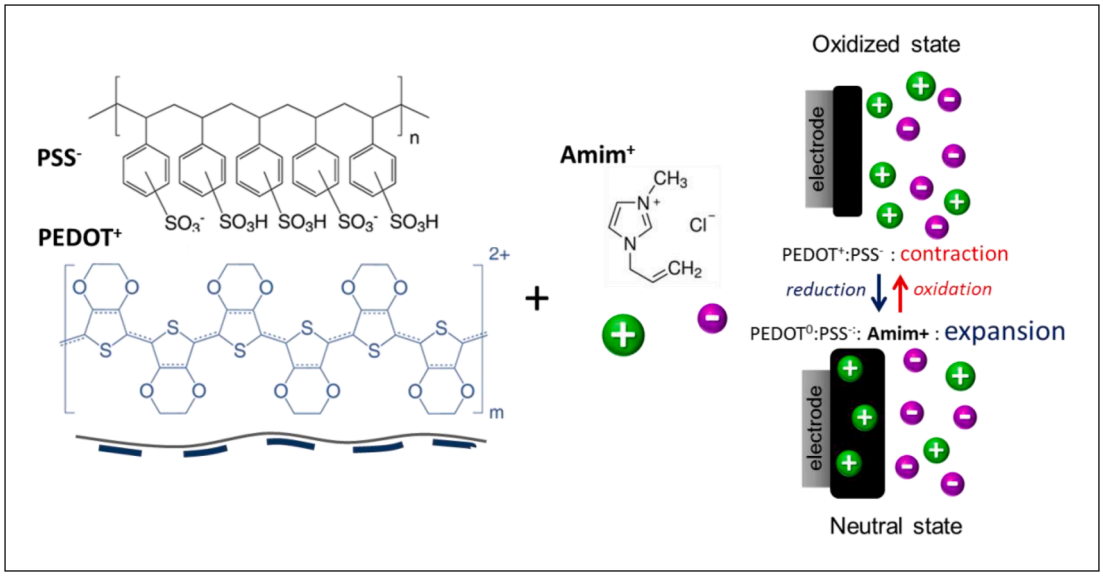

Fig. 2. Oxydation and reduction reactions and associated volume variation of PEDOT:PSS electrodes in the presence of [Amim][Cl] ionic liquid.

2. Materials and methods

It is known that the mechanical properties of starch films highly depend on the amylose content (Lourdin et al., 1995). For this reason, we choose to manufacture EAPs based on pure amylose starch and on potato starch with an amylose/amylopectin ratio of approximately 1/3.

2.1. Manufacturing of trilayer EAP from raw materials

Potato starch was purchased from Roquette (Lestrem, France), pure amylose from Avebe (Veendam, Holland), and 1-Allyl-3-methylimidazolium chloride (98%) from Solvionic (France). PEDOT:PSS 1% aqueous solution (Clevios PH1000) was purchased from Heraeus (Germany) and ethanol (purity 98%) from Sigma Aldrich. All were used as-received without further purification.

The trilayer EAPs are obtained by an origami inspired processes schematized on Fig. 1**b**. The elaboration of electrodes (step 1 in Fig. 1**b**) consisted in spreading the PEDOT:PSS suspension on Teflon templates (1×10 cm^2) and drying at 40 °C during 24 h. A volume of solution 80 µl per cm^2 allowed obtaining PEDOT:PSS electrodes with a thickness a ≈ 10 µm after drying. In order to increase the electronic conductivity, these electrodes were washed with ethanol by immersion during 10 minutes and dried at 40 °C. As illustrated in Fig. 1**b**, step 2 consisted in casting a starch:[Amim][Cl] film onto the dry electrode film. An aqueous solution of potato starch or pure amylose starch was first prepared by dispersing 5 wt.% of polysaccharide in water, and heating at

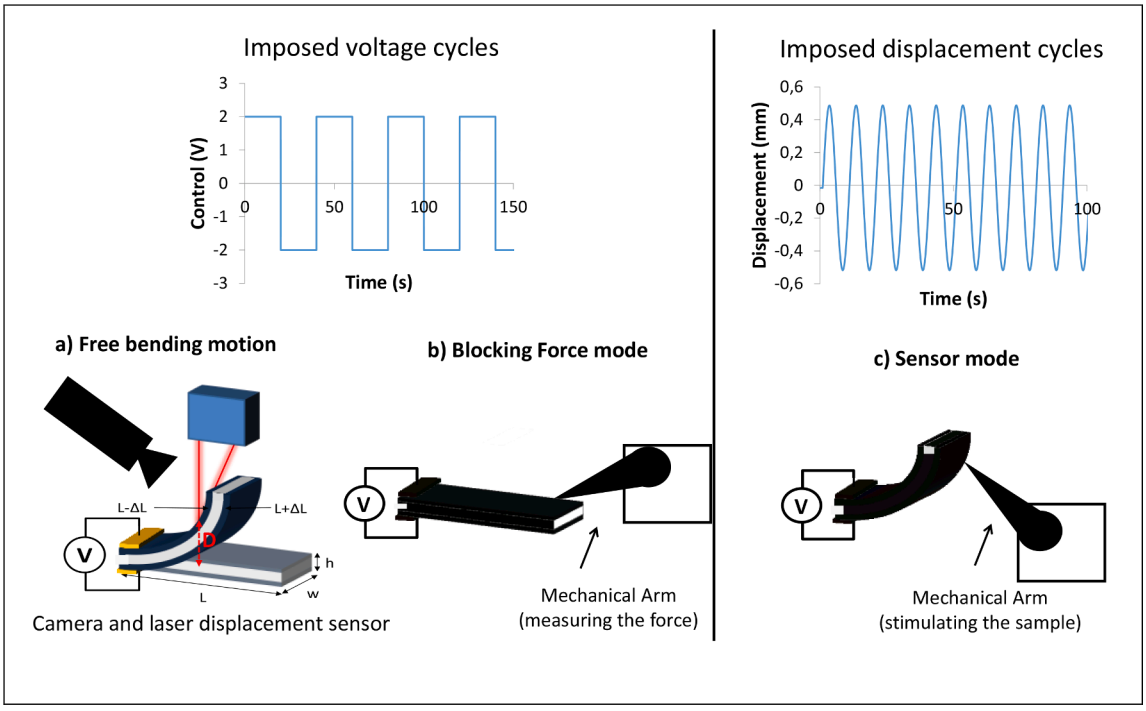

Fig. 3. Experimental setup for testing the EAP trilayer films' electroactive behavior: free bending motion under electric stimulus (a), blocking force mode (b), and sensor mode under mechanical stimulus (c).

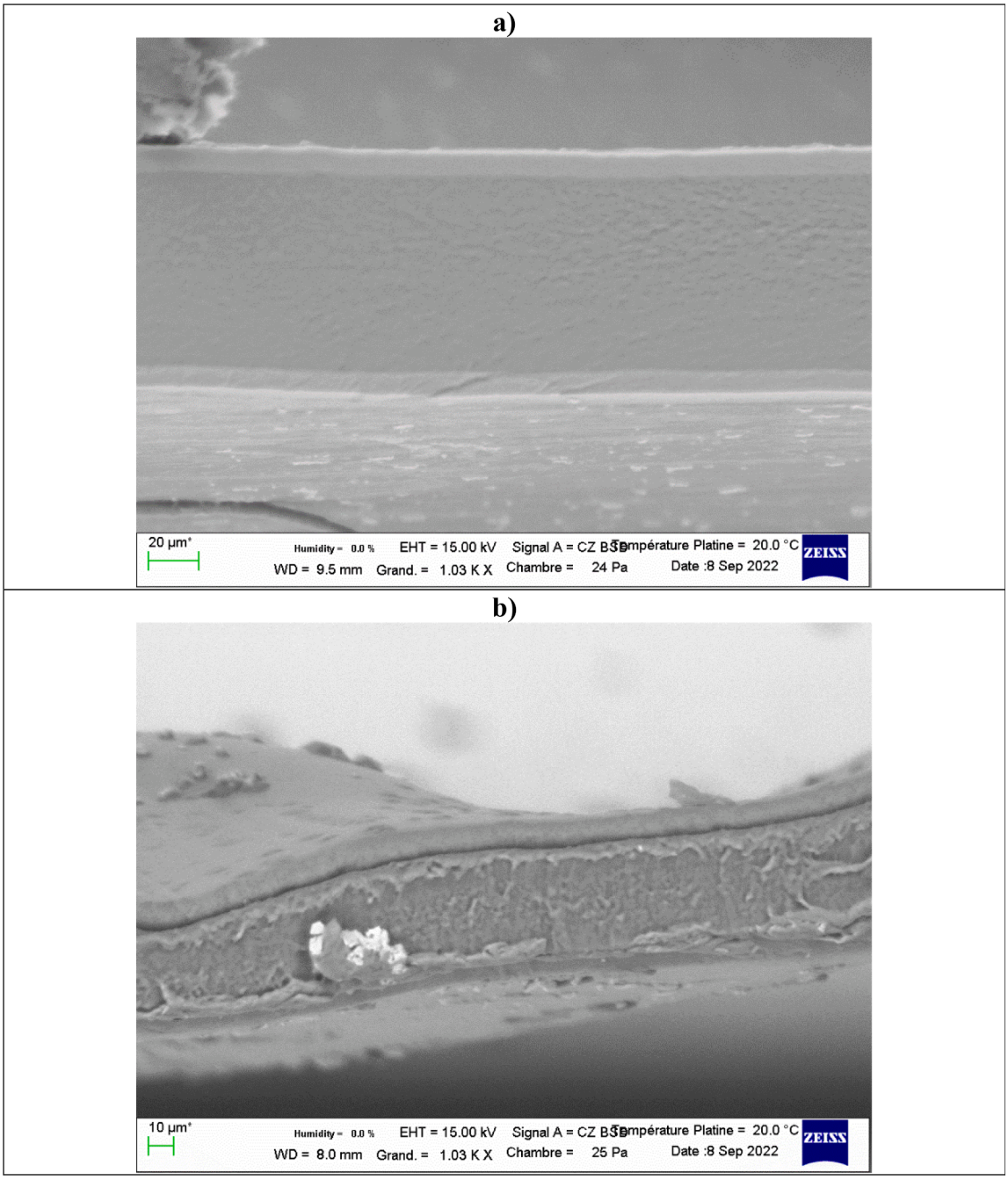

Fig. 4. SEM observation of the EAP films' cross-section (fracture surface of a sample based on potato starch (**a**) and amylose (**b**)).

95 °C under stirring for 5 min. The ionic liquid was added in the solution in order to have a 50:50 starch:[Amim][Cl] w./w. ratio. The solution was spread over the PEDOT:PSS film and dried at 40 °C during 24 h. Adjusting the volume of solution allowed controlling the thickness of this ionic conductive layer (for example, spreading a volume of 50 µl per cm^2 allowed obtaining a Starch:IL layer of approximately b ≈ 50 µm). The last step (step 3 on Fig. 1**b**) takes advantage of the stickiness of the IL rich TPS layer in order to lead to the trilayer structure: It consists in simply folding in half the bilayer film, which sticks on itself, resulting in sheets of total thickness h ≈ 2 (a + b). After a healing time of 24 h, thin parallelepipedic EAP samples of dimensions approximately 20 × 3 mm^2 were cut from the trilayer sheets and stored in sealed plastic bags in order to prevent water uptake before characterizations.

The ionic conductivity of the ICP layer at room temperature (25 ± 1 °C) was evaluated by Electrochemical impedance spectroscopy on potato starch:IL and amylose:IL films. The same casting method as for step 2 was used, except that the substrates were gold electrode in the measurement cell of a VSP potentiostat (Biologic SA). Experiments were carried out in the frequency range from 1 MHz to 1 Hz with an oscillation potential of 10 mV. The ionic conductivity (S/cm) is calculated from the bulk resistance (R) determined as real part of the complex impedance (ohms):

$$\sigma = \frac{d}{R \times A} \tag{1}$$

Where: d the thickness of the sample (cm), and A is the electrode area (cm^2).

2.2. Morphology, water content and dynamic mechanical properties

Scanning Electron Microscopy was used to observe the surface and cross-sectional mor-phology of the EAP using a JEOL 7000F FE-SEM (JEOL, Peabody,USA) at an accelerating voltage of 10 kV. Fracture surfaces were obtained by immersing the trilayer films in liquid nitrogen.

The water content was evaluated by thermogravimetric measurements: samples were heated from 25 °C to 130 °C at 8 °C min^{-1} and maintained at 130 °C during 90 min, reaching a stable mass. The total mass loss was ascribed to water evaporation.

A DMTA apparatus (MKIV, Rheometrics Scientific, USA) was used in the tensile mode with a frequency of 1 Hz and a deformation amplitude of 0.1%. This value is in the range of linear viscoelasticity, and any deviation from this domain during heating was discarded and assumed to be the same for all samples tested. The heating rate was set at 3 °C min^{-1}. The experiments were conducted on the trilayer samples and on single PEDOT:PSS electrodes. No measurements were possible on single starch:LI films which were too sticky.

2.3. Electroactive properties

The experimental setup used for characterizing the electroactive properties of the starch based EAPs schematized on Fig. 3. Samples are mounted side-ways (2 mm clamped, free length 18 mm) between flat gold contacts. Three series of experiments were performed using a VMP potentiostat (Biologic SA) in order to monitor voltage and current:

- A first series of measurements consisted in measuring the free displacement in actuator mode by applying a square wave voltage stimulus (±2 V with steps of 20 seconds) and simultaneously monitoring the current density and the bending motion by a laser displacement sensor (ILD 1401-5, Micro-Epsilon). In order to quantify the electroactive deformation performances, regardless of the dimensions of the sample, it is necessary to calculate the maximal differential strain $\Delta\varepsilon_{max}$ (%) (Sugino et al., 2009):

$$\Delta\varepsilon(\%) = \frac{2D\,x\,h}{L^2 + D^2} x100 \quad (2)$$

Where: D is half of the peak to peak displacement, h is the thickness of the sample (measured with a micrometer), and L = 3 mm is the distance from the fixed end of the actuator to the projection of the laser beam.

The electroactive response rate $\dot{\varepsilon}$ (% × s^{-1}) characterizing the bending motion kinetics, is obtained by dividing $\Delta\varepsilon_{max}$ by the average time Δt_{max} necessary to switch from one maximum displacement to the next one.

- A second series of experiments consisted in measuring the blocking force mode (Fig. 3**b**) by applying the same square wave voltage stimulus (± 2 V with steps of 20 seconds), while measuring the actuating force with a mechanical arm (Muscle Lever Arm 300C from Aurora Scientific). The maximum blocking force F_{max} (mN) can thus be measured.
- Finally, a third series of measurements consisted in measuring the mechanical sensing properties in sensor mode (Fig. 3**c**) by applying a sinusoidal displacement of 0.5 mm with a period of 10 seconds with the mechanical arm (Muscle Lever Arm 300C from Aurora Scientific), while recording both the open-circuit voltage between the electrodes and the necessary mechanical force. The average peak to peak voltage difference ΔV was measured in order to calculate the motion sensor sensitivity ΔV (V/%) and the stiffness k (mN/m) of the EAP, which is related to its apparent bending modulus E_{app} (MPa):

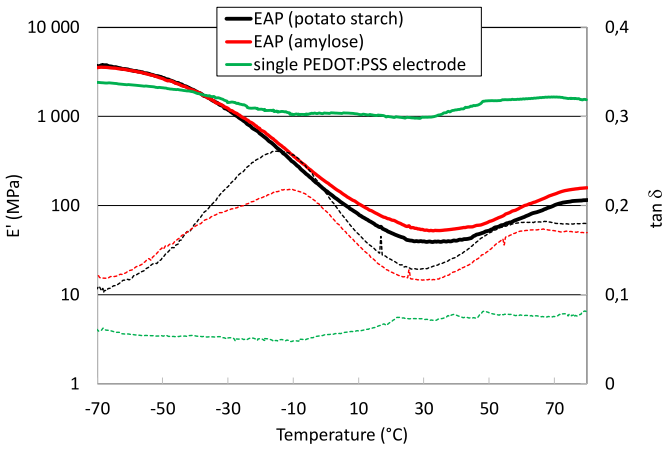

Fig. 5. Dynamic mechanical behavior of the EAP trilayer films based on potato starch or pure amylose, and of a single PEDOT:PSS electrode: Storage modulus (thick lines) and loss angle tangent (dotted lines).

$$E_{app} = \frac{4kL3}{wh3} \quad (3)$$

Where: h is the thickness of the film.

All the above experiments were at least duplicated for each EAP film. Average values and standard deviations were calculated for all the electroactive properties measured.

3. Results and discussion

In the following, we will refer to potato starch and pure amylose as starch and amylose, respectively.

3.1. Structure and thermomechanical properties of trilayer films

During the manufacturing process of EAPs (Fig. 1**b**), the polysaccharide:IL layer casted from aqueous solution (step 2) had a very tacky surface due to the high IL content, so that it efficiently stuck on itself during the origami folding (step 3). Indeed no trace of any folding joint is visible on SEM transverse fracture surfaces (Fig. 4): Only the central starch:IL or amylose:IL (darker grey) and the two external PEDOT:PSS (whiter) can be visually distinguished. Measurements on the SEM images allowed an estimation of the total thickness of the samples: 62 ± 10 µm for the amylose based trilayer films and 87 ± 20 µm for the starch based one. Concurrently, the thicknesses measured directly on the films with a micrometer were typically 100 ± 20 µm. The observation of thicknesses below this range in the SEM may be due to a drying of the films inside the low-pressure microscope cavity.

Additional measurements on the SEM images show that the thicknesses of the upper and lower PEDOT:PSS layers are all equal to approximately 10 µm, while the internal polysaccharide:IL layer thickness is sensibly higher for starch (≈ 54 µm) than for amylose (≈ 44 µm). The water content of the trilayer films measured in TGA was approximately 14% for those based on potato starch and 8% for those based on amylose. Such a difference is consistent with the fact that amylopectin, the major constituent of potato starch, is more hygroscopic than amylose. Moreover, the highly hygroscopic polysaccharide:IL layer is thicker for starch.

The DMTA characterizations show a strong temperature dependence of the EAPs' stiffness (Fig. 5). At -70 °C, both the trilayer films and the single PEDOT:PSS electrode have a glassy behavior with a storage modulus in the GPa range. However, while the mechanical properties of the PEDOT:PSS electrodes remain relatively constant up to +70 °C, a

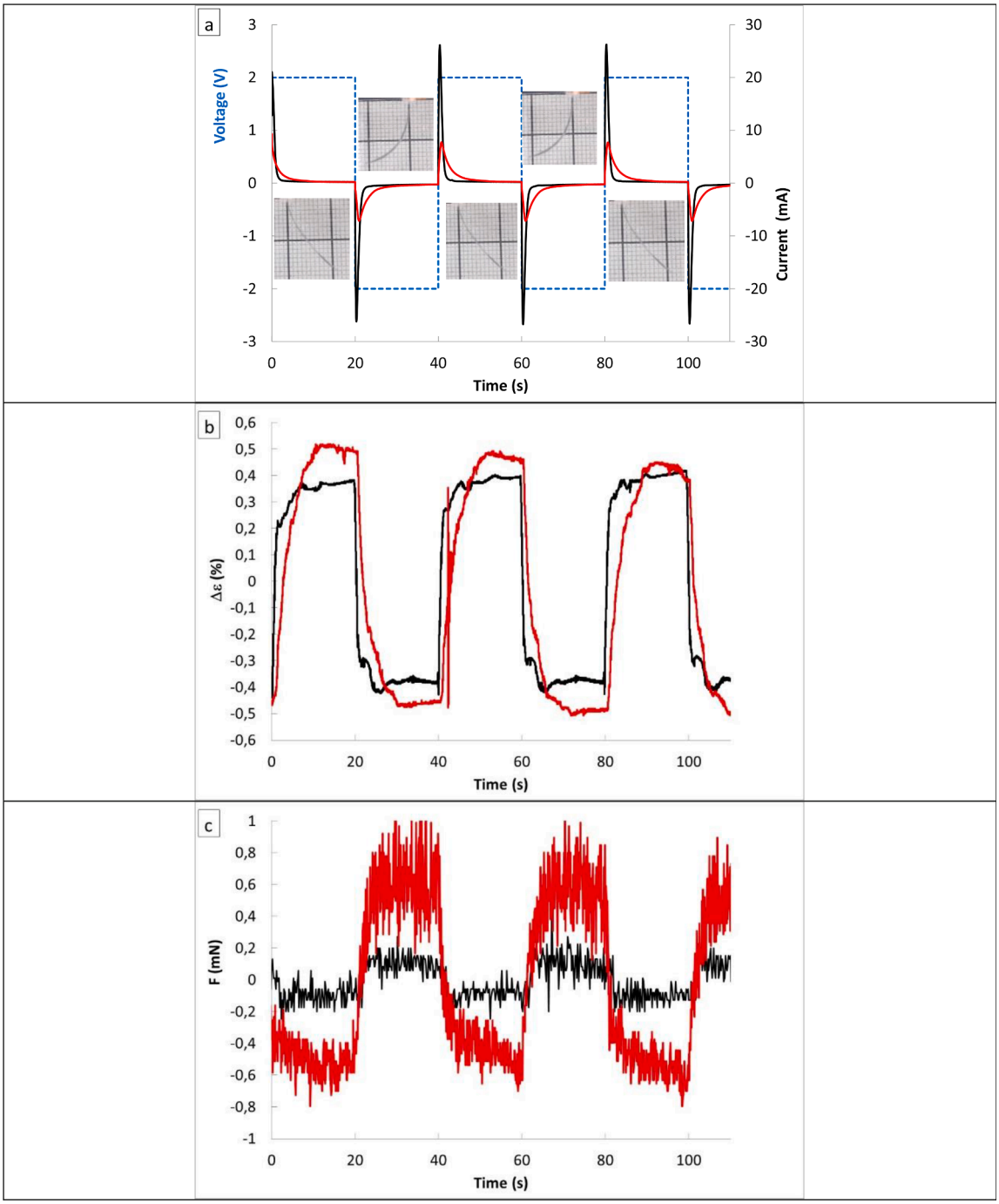

Fig. 6. Typical time dependence of the current (a), the differential strain (b), and the blocking force (c) for an applied step voltage stimulus (dotted lines on a): Curves obtained for potato starch based EAP (black thick lines) and amylose based EAPs (red lines) from free bending motion tests (a,b) and blocking force tests (c). Photographs of maximum free bending motions are shown on (a).

progressive decrease of the trilayer EAPs' storage modulus is observed between -70 °C and +30 °C, reaching a minimum slightly higher for the amylose based EAP ($E'_{30°C} = 53$ MPa), than for the potato starch based EAP ($E'_{30°C} = 40$ MPa). This stiffness decrease can thus be ascribed to the mechanical α relaxation associated to the glass transition of the starch:IL layer. As previously reported for IL plasticized starch, this transition is very broad (Leroy et al., 2012)). The peak of tan δ is situated at around $T_\alpha = -15$ °C and ($T_\alpha = -10$ °C) for the plasticized potato starch layer and the plasticized amylose layer, respectively. Alpha relaxation is very sensitive to water content. Given the very small thickness of the films, it is possible that drying takes place during the DMTA experiment, leading to small water content difference between the samples.

No "rubbery" plateau is observed after the α relaxation, but a stiffening of the EAP films takes place above 30 °C. This storage modulus increase of the trilayer structure may be ascribed to that of the PEDOT:PSS electrode layer. Indeed, the storage modulus of a single electrode increases above 30 °C from 1 GPa to 1.6 GPa. Such a behavior has been previously reported and ascribed to water evaporation, PEDOT:PSS films being highly hygroscopic due to the hydrogen bonding between PSS and water molecules (Zhou et al., 2014). These results indicate that the dynamic tensile mechanical behavior of the EAP trilayer systems at room temperature is mainly dependent on the mechanical properties of

Table 1
Average electroactive performances for 3 samples of each EAP observed in free bending motion, blocking force and sensor modes.

Starch	Free bending motion		Actuator mode		Sensor mode		
	$\Delta\varepsilon$ (%)	$\dot{\varepsilon}$ (% × s^{-1})	F_{max} (mN)	F/W	ΔV (10^{-4} V/%)	k (mN/m)	E_{app} (MPa)
Potato	**0.5** ± 0.1	**0.29** ± 0.18	**0.19** ± 0.01	**18** ± 2	**7.2** ± 0.6	**3,6** ± 0,7	**39** ± 8
Amylose	**0.4** ± 0.1	**0.05** ± 0.04	**1.29** ± 0.23	**182** ± 32	**1.8** ± 0.4	**34.9** ±2,2	**793** ± 51

the thinner but stiffer PEDOT:PSS external layers. The IL plasticized starch or amylose plays a minor role due to its rubbery modulus. Nevertheless, its lower thickness in the amylose based EAP, may explain the higher storage modulus at temperatures above the α relaxation, compared to the starch based EAP. Unfortunately, it was not possible to quantify this modulus, starch:LI films being too sticky and fragile for being manipulated.

3.2. Electroactive properties of the trilayer ionic EAPs

First free motion and blocking force modes were investigated during +2 V/-2 V step voltage of 20 s each, applied between the two PEDOT:PSS electrodes. The current profiles (Fig. 6**a**) show the typical charge and discharge response corresponding to the oxidation/reduction process of PEDOT. After each potential step the current value reaches a peak and then tends to 0 mA when to redox process is reaching completion. It indicates that there is no short-circuit or leakage current between the two electrodes and confirms the success of the origami manufacturing process to prepare trilayer devices. While the peak-to-peak charge consumed for each system (obtained from the integration of current versus time) is similar, ca. 55 mC, the current peak is lower and the current decay is slower in the case of the amylose based EAP. This suggest that similar electroactivity is achieved for the PEDOT:PSS electrodes of both systems but also that actuator based on amylose presents a slower electromechanical behavior.

The ionic conductivity measured on individual ICP layers (casted from solution on gold electrodes and dried at 40 °C during 24 h, as in step 2 of EAP manufacturing process) was similar, slightly higher for the starch based ICP (2.5 10^{-5} S cm^{-1}) than for the amylose based one (2.2 10^{-5} S cm^{-1}). These values are significantly lower than those reported in literature for hydrated films (Wang et al., 2009; Zhang et al., 2017). Therefore, one can expect that in the EAP films, which according to TGA results contain 14% and 8% water, respectively, the ionic conductivity will be significantly higher for the potato starch based system that for the amylose based one, which is consistent with its higher response speed.

The resulting bending deformation of the actuators is simultaneously recorded and the strain difference $\Delta\varepsilon$ is plotted versus time in Fig. 6**b**. First both actuators are presenting a bending deformation confirming the success of the approach. Moreover, they both present similar maximum amplitude of deformation with $\Delta\varepsilon$ values of 0.4% and 0.5%, which is consistent with the similar electrical charge consumed for each system. The actuator made with amylose-based ICP appears however slower with a 6-fold lower response speed $\dot{\varepsilon}$ (Table 1) as expected from the lower ionic conductivity and longer charging time of this system.

The direction of the bending movement indicates that the mechanism is mainly governed by cation movements. Indeed, the actuator bends systematically toward the anode, i.e. the location of the oxidation. It indicates a contraction of the PEDOT:PSS due to the expulsion of $Amim^+$ cations from the electroactive layer during its oxidation and the associated generation of positive charges along the PEDOT backbone. The opposite phenomenon occurs at the cathode with a volume expansion due to the insertion $Amim^+$ cations. This ionic mechanism has been

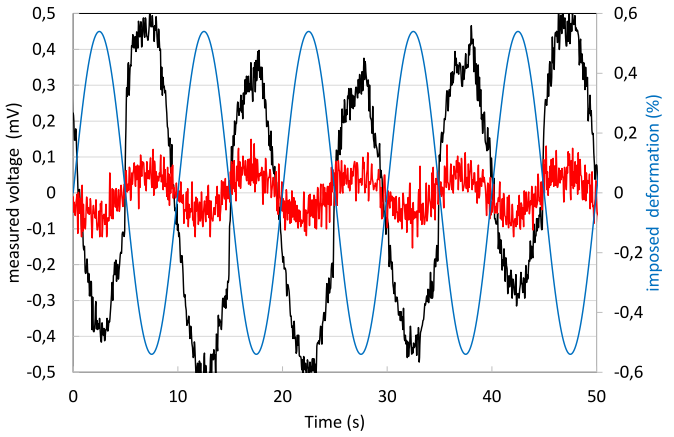

Fig. 7. Response of the EAPs used as sensors, when submitted to a sinusoidal bending deformation (ε= 0.54%, cycle period 10s): potato starch based EAP (black thick lines) and amylose based EAPs (red lines).

reported elsewhere with PEDOT:PSS-based actuators (Rohtlaid et al., 2019) and can be explained by the large presence of the negative polyelectrolyte PSS^- in the electrodes, preventing the insertion of anions and favoring cation exchanges. When measuring the maximum blocking force values F_{max}, it appears that F_{max} is 7 times higher with amylose (Table 1, Fig. 6**c**). This result is consistent with the higher stiffness of the amylose-based EAP compared to the potato starch EAP, as observed in Fig. 5. Taking into account the weight W (mN) of the samples, one can calculate the ratio F/W: The values reported in Table 1 indicate that the stiffer amylose based EAP is able to lift 182 times its weight, while the softer potato starch based EAP lifts only 18 times its weight, which is still remarkable.

The ability of the EAPs to act as sensors was evidenced by submitting the trilayer films to a sinusoidal bending deformation: The generation of a sinusoidal variation of the open-circuit voltage between the clamping gold contacts was observed as a response (Fig. 7). Interestingly, the sensitivity of the sensors are 0.72 and 0.18 mV/% for the potato starch and amylose based EAPs, respectively (Table 1), which is in the same order of magnitude than the 0.7 mV/% of PEDOT:PSS microactuators obtained from fossil-fuel based polymers (Rohtlaid et al., 2019). The higher voltage amplitude for the potato starch based EAP can be ascribed to its higher ionic conductivity and to its lower stiffness: Indeed, the apparent bending modulus E_{app} calculated for the potato starch based EAP (Table 1) is almost equal to the tensile storage modulus measured in DMTA ($E'_{30°C}$ = 40 MPa). This is not the case for the amylose based EAP, for which $E_{app} \approx 15 \times E'_{30°C}$. It results in a ten-fold higher bending stiffness for amylose based EAPs.

This would suggest a strong mechanical anisotropy for amylose based EAPs. However, one should remind that DMTA experiments may involve drying, resulting in a small water content difference between the samples. This is not the case for the room temperature sensor mode measurements, during which the water content in the starch based EAPs is significantly higher than that of the amylose based ones, according to TGA measurements. Therefore, the softening of the PEDOT:PSS electrodes due to water uptake should be higher in the former, resulting in lower values of E_{app}.

Anyhow, it points out the fact that electroactive properties of IL plasticized starch based EAPs are sensitive to water content. This sensitivity should be the subject of future works.

The above results suggest that IL plasticized starch ICPs may play an important role in the development of sustainable biobased smart polymeric devices, able to compete with petroleum based systems in the 21st century, and bringing new possibilities in terms of manufacturing processes. However, this will also require: i) the development of biobased and/or biodegradable ILs and ECPs; and ii) further studying the impact

of this replacement of petroleum-based materials on the stability (in presence of moisture in particular) and durability (in case of eventual starch retrogradation for example) of the performances of the actuators and/or sensors.

4. Conclusions

The use of ionic liquid (IL) plasticized starch as an Ionically Conductive Polymer (ICP) was shown to be a promising alternative to fossil fuel based ICP for the manufacturing of air working (≈ 100 μm thick) symmetrical trilayer Electroactive Polymer (EAP) films able to work as bending actuators, or as sensors under applied bending deformation. The water solubility of the starch/IL mixture and its stickiness after casting as films allowed the design of a solvent free, origami inspired casting/folding process for its assembly with PEDOT:PSS electron conducting polymer (ECP) films.

The results obtained with potato starch and pure amylose starch show that the electroactive properties can be significantly modulated by the botanical origin and characteristics of starch, in order to reach performances comparable to fossil-fuel based polymers systems.

Following this proof of concept, future works should focus on how electroactive properties are influenced by water uptake, and may evolve upon aging due to the possible retrogradation of starch over time. Last but not least, starch being biodegradable, evaluating the influence of its use on the end of life and environmental impact of the EAPs will be of primary interest.

Declaration of Competing Interest

The authors declare that they have no known competing financial interests or personal relationships that could have appeared to influence the work reported in this paper.

Data availability

Data will be made available on request.

Aknowledgments

The authors would like to acknowledge financial support from the French Ionic Liquids and Polymers network funded by CNRS (GDR 3585 LIPS)

References

Alemu, D., Wei, H.-Y., Ho, K.-C., & Chu, C.-W. (2012). Highly conductive PEDOT:PSS electrode by simple film treatment with methanol for ITO-free polymer solar cells. *Energy & Environmental Science, 5*(11), 9662. https://doi.org/10.1039/c2ee22595f

Arrieta, Palencia, & Pestana. (2018). New composite biopolymer with conductive properties obtained from cassava and poly starch (3, 4-Ethylenedioxythiophene). *Indian Journal of Science and Technology, 11*(2), 1–10. https://doi.org/10.17485/ijst/2018/v11i2/117345

Bar-Cohen, Y. (2002). Electroactive polymers as artificial muscles: A review. *Journal of Spacecraft and Rockets, 39*(6), 822–827. https://doi.org/10.2514/2.3902

Bar-Cohen, Y., & Anderson, I. A. (2019). Electroactive polymer (EAP) actuators—Background review. *Mechanics of Soft Materials, 1*(1), 5. https://doi.org/10.1007/s42558-019-0005-1

Bar-Cohen, Y., & Zhang, Q. (2008). Electroactive polymer actuators and sensors. *MRS Bulletin, 33*(3), 173–181. https://doi.org/10.1557/mrs2008.42

Finkenstadt, V. L. (2005). Natural polysaccharides as electroactive polymers. *Applied Microbiology and Biotechnology, 67*(6), 735–745. https://doi.org/10.1007/s00253-005-1931-4

Finkenstadt, V. L., & Willett, J. L. (2004). Electroactive materials composed of starch. *Journal of Polymers and the Environment, 12*(2), 43–46.

Finkenstadt, V., & Willett, J. L. (2005). Preparation and characterization of electroactive biopolymers. *Macromolecular Symposia, 227*(1), 367–372. https://doi.org/10.1002/masy.200550937

Groenendaal, L., Jonas, F., Freitag, D., Pielartzik, H., & Reynolds, J. (2000). Poly(3,4-ethylenedioxythiophene) and its derivatives: past, present, and future. *Advanced Materials*, 481–494.

Leroy, E., Jacquet, P., Coativy, G., Reguerre, A. L., & Lourdin, D. (2012). Compatibilization of starch-zein melt processed blends by an ionic liquid used as plasticizer. *Carbohydrate Polymers, 89*(3), 955–963. https://doi.org/10.1016/j.carbpol.2012.04.044

Lourdin, D., Valle, G. D., & Colonna, P. (1995). Influence of amylose content on starch films and foams. *Carbohydrate Polymers, 27*(4), 261–270. https://doi.org/10.1016/0144-8617(95)00071-2

Ma, X., Yu, J., & He, K. (2006). Thermoplastic starch plasticized by glycerol as solid polymer electrolytes. *Macromolecular Materials and Engineering, 291*(11), 1407–1413. https://doi.org/10.1002/mame.200600261

Maziz, A., Concas, A., Khaldi, A., Stålhand, J., Persson, N.-K., & Jager, E. W. H. (2017). Knitting and weaving artificial muscles. *Science Advances, 3*(1), Article e1600327. https://doi.org/10.1126/sciadv.1600327

Melling, D., Martinez, J. G., & Jager, E. W. H. (2019). Conjugated polymer actuators and devices: Progress and opportunities. *Advanced Materials, 31*(22), Article 1808210. https://doi.org/10.1002/adma.201808210

Mirfakhrai, T., Madden, J. D. W., & Baughman, R. H. (2007). Polymer artificial muscles. *Materials Today, 10*(4), 30–38. https://doi.org/10.1016/S1369-7021(07)70048-2

Y. E.Á. A.J. A. Núñez, D, Arrieta, A, Segura, B, & Bertel, H (2016). Synthesis of an air-working trilayer artificial muscle using a conductive cassava starch biofilm (manihot esculenta, cranz) and polypyrrole (PPy) *Journal of Physics: Conference Series, 687*, Article 012042. https://doi.org/10.1088/1742-6596/687/1/012042

Rohtlaid, K., Nguyen, G. T. M., Soyer, C., Cattan, E., Vidal, F., & Plesse, C. (2019). Poly(3,4-ethylenedioxythiophene):Poly(styrene sulfonate)/polyethylene oxide electrodes with improved electrical and electrochemical properties for soft microactuators and microsensors. *Advanced Electronic Materials, 5*(4), Article 1800948. https://doi.org/10.1002/aelm.201800948

Sankri, A., Arhaliass, A., Dez, I., Gaumont, A. C., Grohens, Y., Lourdin, D., Pillin, I., Rolland-Sabate, A., & Leroy, E. (2010). Thermoplastic starch plasticized by an ionic liquid. *Carbohydrate Polymers, 82*(2), 256–263. https://doi.org/10.1016/j.carbpol.2010.04.032

Sugino, T., Kiyohara, K., Takeuchi, I., Mukai, K., & Asaka, K. (2009). Actuator properties of the complexes composed by carbon nanotube and ionic liquid: The effects of additives. *Sensors and Actuators B: Chemical, 141*(1), 179–186. https://doi.org/10.1016/j.snb.2009.06.002

Wang, N., Zhang, X. X., Liu, H. H., & He, B. Q. (2009). 1-Allyl-3-methylimidazolium chloride plasticized-corn starch as solid biopolymer electrolytes. *Carbohydrate Polymers, 76*(3), 482–484. https://doi.org/10.1016/j.carbpol.2008.11.005

Zhang, B., Xie, F., Shamshina, J. L., Rogers, R. D., McNally, T., Wang, D. K., Halley, P. J., Truss, R. W., Zhao, S., & Chen, L. (2017). Facile preparation of starch-based electroconductive films with ionic liquid. *ACS Sustainable Chemistry & Engineering, 5*(6), 5457–5467. https://doi.org/10.1021/acssuschemeng.7b00788

Zhao, D., Wang, C., Luo, X., Fu, X., Liu, H., & Yu, L. (2015). Morphology and phase transition of waxy cornstarch in solvents of 1-allyl-3-methylimidazolium chloride/water. *International Journal of Biological Macromolecules, 78*, 304–312. https://doi.org/10.1016/j.ijbiomac.2015.04.020

Zhou, J., Anjum, D. H., Chen, L., Xu, X., Ventura, I. A., Jiang, L., & Lubineau, G. (2014). The temperature-dependent microstructure of PEDOT/PSS films: Insights from morphological, mechanical and electrical analyses. *J. Mater. Chem. C, 2*(46), 9903–9910. https://doi.org/10.1039/C4TC01593B